Nuclear Activity in Galaxies Across Cosmic Time
Proceedings IAU Symposium No. 356, 2019
M. Pović, P. Marziani, J. Masegosa, H. Netzer, S. H. Negu & S. B. Tessema, eds.
doi:10.1017/S1743921320002550

Hypercat - hypercube of AGN tori

Robert Nikutta[1], Enrique Lopez-Rodriguez[2], Kohei Ichikawa[3,4], Nancy A. Levenson[5] and Christopher C. Packham[6,7]

[1]NSF's National Optical-Infrared Astronomy Research Laboratory
950 N Cherry Avenue, Tucson, AZ 85719, USA
email: nikutta@noao.edu

[2]SOFIA Science Center, NASA Ames Research Center, Moffett Field, CA 94035, USA

[3]Frontier Research Institute for Interdisciplinary Sciences, Tohoku University, Sendai 980-8578, Japan

[4]Astronomical Institute, Tohoku University, Aramaki, Aoba-ku, Sendai, Miyagi 980-8578, Japan

[5]Space Telescope Science Institute, Baltimore, MD 21218, USA

[6]Department of Physics & Astronomy, University of Texas at San Antonio, One UTSA Circle, San Antonio, TX 78249, USA

[7]National Astronomical Observatory of Japan, 2-21-1 Osawa, Mitaka, Tokyo 181-8588, Japan

Abstract. We introduce Hypercat, a large set of 2-d AGN torus images computed with the state-of-the-art clumpy radiative transfer code Clumpy. The images are provided as a 9-dimensional hypercube, in addition to a smaller hypercube of corresponding projected dust distribution maps. Hypercat also comprises a software suite for easy use of the hypercubes, quantification of image morphology, and simulation of synthetic observations with single-dish telescopes, interferometers, and Integral Field Units. We apply Hypercat to NGC 1068 and find that it can be spatially resolved in Near- and Mid-IR, for the first time with single-dish apertures, on the upcoming generation of 25–40m class telescopes. We also find that clumpy AGN torus models within a range of the parameter space can explain on scales of several parsec the recently reported polar elongation of MIR emission in several sources, while not upending basic assumptions about AGN unification.

Keywords. galaxies: active, galaxies: nuclei, galaxies: Seyfert, infrared: galaxies radiative transfer, instrumentation: high angular resolution, instrumentation: interferometers, methods: data analysis, techniques: high angular resolution

1. Introduction

Unification of active galactic nuclei (AGN) (e.g. Antonucci 1993; Urry & Padovani 1995) has explained much of the dichotomy between type 1 and type 2 AGN, by simply assuming an axially symmetric, anisotropic, dusty obscurer – a torus – and its orientation to the observer's line of sight (LOS). Complications were brought about by ever-improving observations, and these required modifications to the simple torus picture; the field has mostly converged on very compact (e.g. Jaffe *et al.* 2004; Gallimore *et al.* 2016) and clumpy (e.g. Nenkova *et al.* 2008a,b; Markowitz *et al.* 2014) distributions of dust and molecular gas surrounding the accreting supermassive black hole. The structure and dynamics of the molecular matter within the innermost few parsecs appear to be rather complex (Impellizzeri *et al.* 2019; Combes *et al.* 2019).

In the simple torus picture, most of the circum-nuclear dust is concentrated, by design, toward the torus equatorial plane, and that is where most of the dust emission is expected to emerge. Recent observation yet again are pushing the envelope; in several nearby

sources, where high-spatial resolution interferometric or photometric observations are possible, the MIR emission shows clear signs of elongation along the system axis, not along its equatorial plane (e.g. Hönig *et al.* 2013; López-Gonzaga *et al.* 2016; Asmus 2019). At first this seems incompatible with torus-based unification. Modified models have been proposed to explain these observations e.g. as an inversion of the cloud distribution from toroidal to bi-conical (Hönig & Kishimoto 2017), or through interplays between a tilted accretion disk that anisotropically illuminates a hollow, bi-conical, dusty wind (Stalevski *et al.* 2017). Tristram *et al.* (2014) suggested for the case of Circinus that the elongation is due to seeing the inner wall of a torus funnel slightly tilted toward us.

Today's single-dish telescopes can not resolve the central tens of parsecs even in the closest sources. Second-generation IR interferometers such as *VLTI* combine light from only two telescopes, thus do not achieve phase closure. This fundamentally prevents image reconstruction. However, the observed visibilities as function of baseline, position angle, and wavelength can be compared to models of brightness distribution. The most common approach so far has been to model a synthetic brightness distribution with a linear combination of 2d Gaussian components. Even in its simplest incarnation, this approach required no fewer than 18 free parameters in the case of Circinus (Tristram *et al.* 2014). The upcoming class of 25–40m giant telescopes (GMT, TMT, ELT) will for the first time deliver model-free resolved imagery of the central parsecs in nearby AGN at IR wavelengths. It is clear that further progress must come from modeling the observed brightness distribution as the result of radiative transfer through the underlying physical, 3d, distribution of dust. Only inferences following this approach will be able to constrain the actual geometry and physics and parsec scales. Hypercat's image and dust cubes are developed precisely for that purpose.

2. Hypercubes of light and dust

Model SEDs of AGN emission are abundant and have been used with success in the literature, but studies using resolved model images remain in their infancy. First, because until recently no spatially resolved data were available and, second, because computation, storage, and processing of image sets with sufficient parameter coverage are prohibitively expensive. *VLTI* and *ALMA*, and upcoming facilities such as *TMT*, *GMT* and *ELT* have or will alleviate the first problem. Hypercat is designed to break the second barrier.

It is a user-friendly software that hides the complexity of handling very large multi-dimensional hypercubes of data. Hypercat can generate an image of the torus emission (or a dust map) for any combination of parameters via multilinear interpolation in fractions of a second. It can also simulate observations of these images with single-dish telescopes. These include PSF convolution (provided by the user or computed by Hypercat), image transformations (e.g. rotation, scaling, resampling), noise addition to a signal-to-noise ratio (SNR), and deconvolution. Interferometry can also be simulated for a set of (u,v) points. Furthermore, spatially resolved maps of spectral properties can be analyzed akin to integral-field-units (IFU). Finally, a module to compute image morphology quantifiers completes the Hypercat software. Hypercat is open-source, written in Python, and will be publicly available shortly[1]. We also release our image hypercubes[2] generated with Clumpy, which we describe below.

2.1. *Model hypercubes*

Clumpy models the distribution of dust clouds around an AGN as an axisymmetric function of cloud number density, requiring four free parameters – ratio of outer to inner

[1] Please visit https://clumpy.org/
[2] Available at: ftp://ftp.noao.edu/pub/nikutta/hypercat/

https://doi.org/10.1017/S1743921320002550 Published online by Cambridge University Press

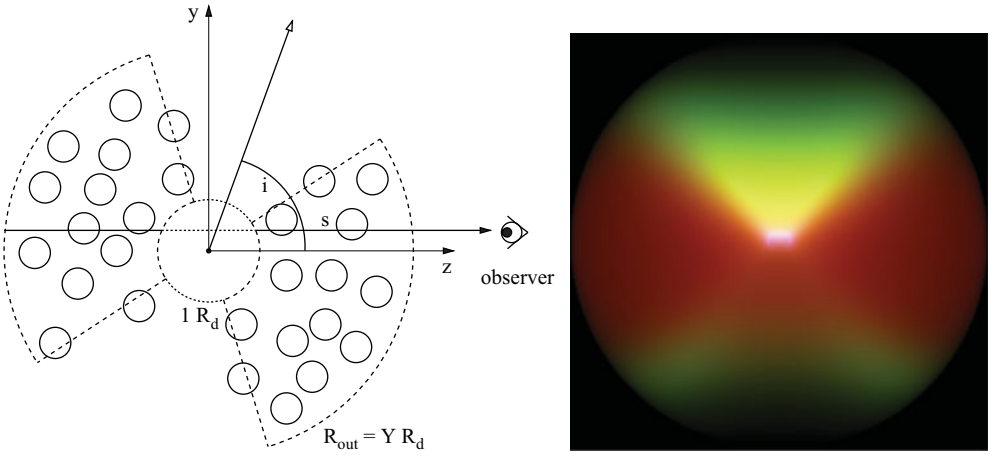

Figure 1. *Left:* Vertical cut through a schematic toroidal cloud distribution. The torus angular edge is soft, i.e. cloud number falls off from the mid-plane like a Gaussian. *Right:* What an observer in the left panel might see; composite of three CLUMPY brightness maps at 4.6, 10, 25 μm (blue, green, red). The relative contributions of all maps were equalized for clarity. The model has parameters $\sigma = 30$ deg, $i = 80$ deg, $Y = 20$, $\mathcal{N}_0 = 7$, $q = 0.1$, and $\tau_V = 75$. In this configuration the MIR emission occurs predominantly from polar directions, i.e. from the inner walls of the torus cone (green color).

torus radii, Y; mean number of clouds along a radial ray in the equatorial plane, $\mathcal{N}_0$; exponent q of the radial power-law profile $1/r^q$ (with r the distance); and torus angular width σ measured in degrees from the equatorial plane. In addition, the viewing angle i between the system axis and the observer's LOS, and the wavelength λ are required to quantify a model. Dust radiative transfer calculations performed by CLUMPY result in an image $I(x, y)$ discretized along axes x and y. Figure 1 shows on the left a schematic view of a cloud distribution and the propagation of photons along the LOS. On the right is what an observer will see – in this case a composite image of three distinct wavelengths.

A hypercube of all computed images is 9-dimensional. Our sampling of parameters yields 336,000 combinations, times 25 wavelengths between 1.2 and 945μm. Together with the ≈ 2000 times smaller corresponding dust maps, the hypercubes contain 2.45×10^{11} values (when storing half-images), at a resolution of six pixels per dust sublimation radius. This corresponds to 913/271 GB of raw/compressed storage. Computation consumed 3.2 years of CPU time. Downloading and storage are tractable with a broad-band internet connection and storage capacities on modern laptops, but handling a data hypercube of this size is not. HYPERCAT was designed to jump this entry barrier.

2.2. *Software suite*

The HYPERCAT software suite comprises Python modules, accessible through a high-level API suitable for most users. A low-level set of functions allows to operate on images more directly. A simple GUI is also provided, which allows image generation for any parameter combination, saving to a FITS file for further processing, or displaying of images in DS9[1] directly. A user manual and example Jupyter notebooks facilitate a quick start with HYPERCAT.

[1] SAO DS9: http://ds9.si.edu/

https://doi.org/10.1017/S1743921320002550 Published online by Cambridge University Press

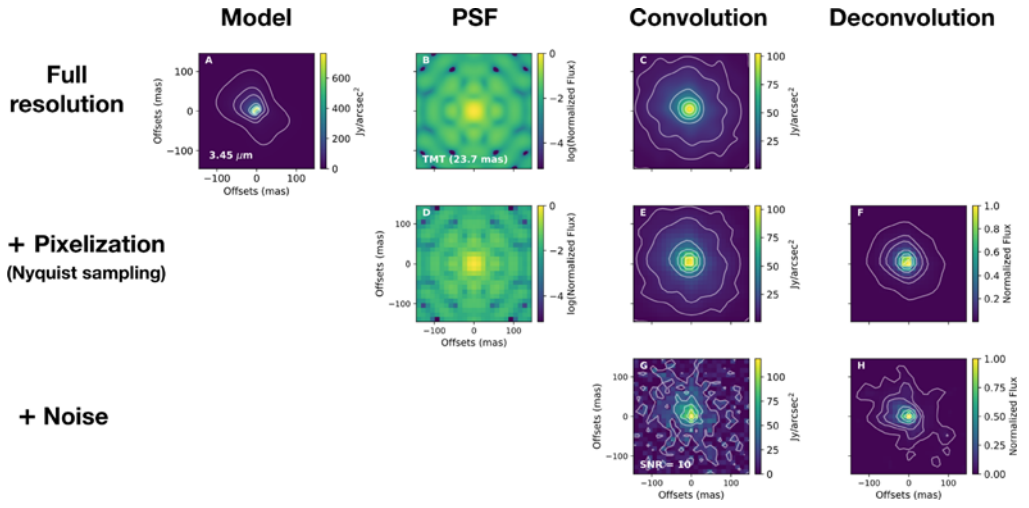

Figure 2. HYPERCAT step-by-step process to obtain synthetic observations of the 2-d dust emission distribution using CLUMPY models. *(A)* Dust emission image at 3.45 μm of NGC 1068 produced by a CLUMPY model using the best-fit parameters obtained via SED fitting by Lopez-Rodriguez *et al.* (2018) ($\sigma = 45°$, $Y = 18$, $\mathcal{N}_0 = 4$, $q = 0.08$, $\tau_V = 70$, $i = 75°$). *(B)* PSF at 3.45 μm estimated using the pupil image of the *TMT* at full resolution (1.21 mas). *(C)* Convolved image using the full resolution dust emission (A) and PSF (B) images. *(D)* PSF pixelated at the Nyquist sampling of the *TMT* at 3.45 μm. Pixel scale is 11.6 mas. *(E)* Pixelated dust emission image of NGC 1068 at same pixel scale as D. *(F)* Deconvolved dust emission image using D and E. *(G)* Gaussian noise with SNR = 10 at the peak pixel was applied to E. *(H)* Deconvolved image using the pixelated PSF D and noisy image G.

3. Application to NGC 1068

We applied HYPERCAT to NGC 1068, a nearby AGN with very good data available from many campaigns. Applying best-fit CLUMPY model parameters found by Lopez-Rodriguez *et al.* (2018) through detailed SED fitting, HYPERCAT interpolated the corresponding images at all wavelengths of interest. Figure 2 shows in panel (A) the brightness map at 3.45μm, and outlines how synthetic observations can be simulated step-by-step in HYPERCAT using this input image. The steps include convolution with a PSF (provided by user or computed by HYPERCAT from telescope pupil images), addition of noise to a specified SNR, and image deconvolution. A major result is that the upcoming generation of extremely large telescopes will indeed resolve the circum-nuclear dust emission in several AGN in the L, M and N bands, as is evident from e.g. panel (H) in Fig. 2.

HYPERCAT can also simulate simple interferometric observations, and analyze spectrally-resolved observations per-pixel, akin to IFUs. We will publish these results in a forthcoming paper (Nikutta et al., in prep.).

4. Morphology

We developed a mechanism based on image moments to quantify morphological properties of images generated by CLUMPY, which allow us to measure the extension of an emission region in x and y directions independently, to measure the extension direction and amplitude, and other useful morphological properties. We investigated for the case of NGC 1068 which parameter variations produce image elongations compatible with those reported in observations. Figure 3 shows the elongation e, defined as the ratio of

https://doi.org/10.1017/S1743921320002550 Published online by Cambridge University Press

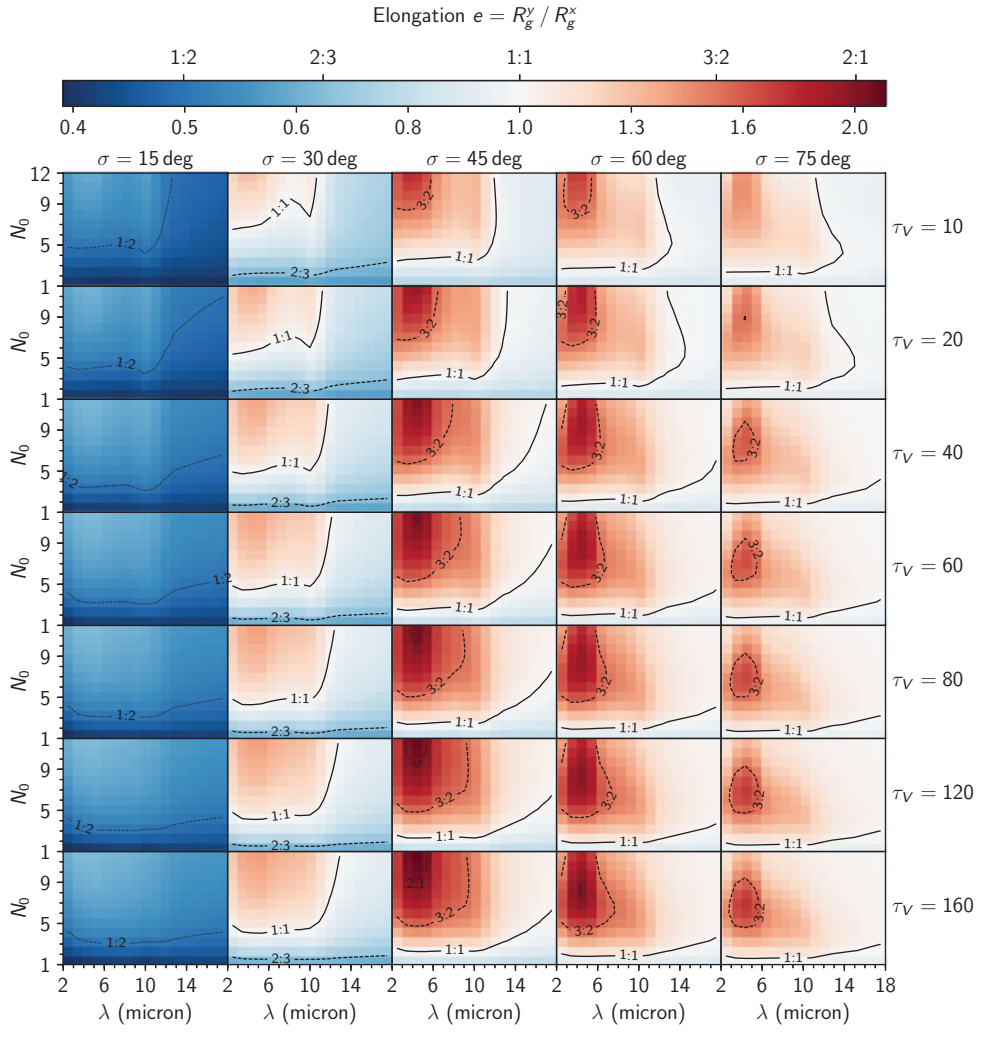

Figure 3. Image elongation e as function of varied parameters, shown as heatmaps. Red colors show elongation in y-direction (polar), blue colors in x-direction (equatorial). Some best-fit parameters values from SED fitting of NGC 1068 are held fixed, i.e. $i = 75$ degrees, $q = 0.08$, $Y = 18$, while all other parameters vary as indicated. All panels are normalized to the same range and are logarithmically stretched separately for values smaller/greater than 1.0 (see color bar). Contour lines show aspect ratios 1:1 (solid), 2:3 and 3:2 (dashed), 2:1 and 1:2 (dotted), also marked on the colorbar (upper tickmarks).

so-called gyration radii in both directions, as a function of model parameters and wavelengths. Dark-red regions in the graphs indicate parameter spaces that produce strong polar elongations of 2:1 and higher.

5. Summary

HYPERCAT provides *(i)* a very large hypercube of AGN torus images computed with CLUMPY, *(ii)* the corresponding dust maps, and *(iii)* a software suite to make easy use of the maps, and to simulate observations with single-dish telescopes, interferometers, and IFUs. It also comprises a module to estimate various image morphology parameters. We have applied HYPERCAT to the case of NGC 1068 in an attempt to derive the torus

https://doi.org/10.1017/S1743921320002550 Published online by Cambridge University Press

geometry, and to quantify the emerging morphology of the observed brightness distributions. We find that in this case, and for a range of model parameters, clumpy tori can indeed produce emission maps strongly elongated in the polar directions of the system, requiring only a small tilt of the torus axis toward the observer. This affords a view of the MIR emission coming off the inner torus walls. The elongations can reach up to several pc in real systems, which can explain much of the very-high resolution data from e.g. VLTI. It is likely not sufficient, by the nature of model sizes, to explain MIR elongations on scales of tens of pc; these are presumably caused by other mechanisms, e.g. by a dusty outflow.

References

Antonucci, R. 1993, *ARA&A*, 31, 473, doi: 10.1146/annurev.aa.31.090193.002353
Asmus, D. 2019, *MNRAS*, 2220, doi: 10.1093/mnras/stz2289
Combes, F., García-Burillo, S., Audibert, A., *et al.* 2019, *A&A*, 623, A79, doi: 10.1051/0004-6361/201834560
Gallimore, J. F., Elitzur, M., Maiolino, R., *et al.* 2016, *ApJL*, 829, L7, doi: 10.3847/2041-8205/829/1/L7
Hönig, S. F. & Kishimoto, M. 2017, *ApJL*, 838, L20, doi: 10.3847/2041-8213/aa6838
Hönig, S. F., Kishimoto, M., Tristram, K. R. W., *et al.* 2013, *ApJ*, 771, 87, doi: 10.1088/0004-637X/771/2/87
Impellizzeri, C. M. V., Gallimore, J. F., Baum, S. A., *et al.* 2019, *ApJL*, 884, L28, doi: 10.3847/2041-8213/ab3c64
Jaffe, W., Meisenheimer, K., Röttgering, H. J. A., *et al.* 2004, *Nature*, 429, 47, doi: 10.1038/nature02531
López-Gonzaga, N., Burtscher, L., Tristram, K. R. W., Meisenheimer, K., & Schartmann, M. 2016, *A&A*, 591, A47, doi: 10.1051/0004-6361/201527590
Lopez-Rodriguez, E., Fuller, L., Alonso-Herrero, A., *et al.* 2018, *ApJ*, 859, 99, doi: 10.3847/1538-4357/aabd7b
Markowitz, A. G., Krumpe, M., & Nikutta, R. 2014, *MNRAS*, 439, 1403, doi: 10.1093/mnras/stt2492
Nenkova, M., Sirocky, M. M., Ivezić, Ž., & Elitzur, M. 2008a, ApJ, 685, 147, doi: 10.1086/590482
Nenkova, M., Sirocky, M. M., Nikutta, R., Ivezić, Ž., & Elitzur, M. 2008b, *ApJ*, 685, 160, doi: 10.1086/590483
Stalevski, M., Asmus, D., & Tristram, K. R. W. 2017, *MNRAS*, 472, 3854, doi: 10.1093/mnras/stx2227
Tristram, K. R. W., Burtscher, L., Jaffe, W., *et al.* 2014, *A&A*, 563, A82, doi: 10.1051/0004-6361/201322698
Urry, C. M., & Padovani, P. 1995, *PASP*, 107, 803, doi: 10.1086/133630